Turkish Journal of Chemistry
http://journals.tubitak.gov.tr/chem/
Research Article

Turk J Chem
(2014) 38: 725 – 738

doi:10.3906/kim-1308-11

Binding of flavanone with β-CD/ctDNA: a spectroscopic investigation

Chandrasekaran SOWRIRAJAN, Sameena YOUSUF, Muthu Vijayan Enoch ISRAEL VIJAYARAJ*
Department of Chemistry, Karunya University, Coimbatore, Tamil Nadu, India

Received: 03.08.2013 • **Accepted:** 13.02.2014 • **Published Online:** 15.08.2014 • **Printed:** 12.09.2014

Abstract: The inclusion complexation of flavanone with β-cyclodextrin was studied by ultraviolet absorption, steady state fluorescence, time-resolved fluorescence, and 2D ROESY nuclear magnetic resonance spectroscopic techniques. A 1:1 stoichiometric ratio was determined for the inclusion of flavanone with β-cyclodextrin. The Stern–Volmer constant for the accessible fraction of the binding of flavanone with β-cyclodextrin, and the binding constant for the flavanone–β-cyclodextrin complex are reported. The flavanone– β-cyclodextrin inclusion complex was characterized by 2D ROESY NMR spectroscopy. The binding of flavanone with ctDNA and the effect of β-cyclodextrin on the binding of flavanone to ctDNA were studied by absorption and fluorescence techniques. Binding constants are reported for the binding of flavanone with ctDNA and flavanone– β-cyclodextrin with ctDNA. The mode of binding of flavanone to DNA and formation of inclusion complex with β-cyclodextrin are proposed, supported by molecular modeling. The studies imply that β-cyclodextrin acts as carrier of flavanone for binding with DNA.

Key words: Flavanone, β-cyclodextrin, fluorescence, ctDNA binding, 2D ROESY

1. Introduction

Cyclodextrins (CDs) are bucket-shaped cyclic oligosaccharides, mostly consisting of 6, 7, and 8 glucose units for α-CD, β-CD, and γ-CD, respectively. They have nonpolar cavities capable of accommodating a large variety of molecules to form inclusion complexes.[1] Release of molecules from the cyclodextrin-bound condition and encapsulation of toxic groups lead to widespread applications in pharmaceutical chemistry, food technology, and analytical chemistry.[2–7] Efforts have been spurred to understand the inclusion complexation between CDs and several types of guest molecules. The encapsulation alters the properties of the guest molecule, which is protected against the aqueous medium from light, oxidants, or reactive attacks. A large number of studies found in the literature regarding the CD formulation of drugs have been carried out from a biomedical standpoint.[8–10] The stoichiometry, the binding constant, and the geometry of the complex are necessary to draw a complete picture of the driving forces governing the small molecule–CD interaction.

Flavanones, originally isolated from natural sources, are an important class of naturally occurring bioactive compounds. Flavanone derivatives have been reported to possess a variety of biological activities including anticancer,[11] antimitotic,[12] antiinflammatory,[13] antimalarial,[14] antiangiogenic,[15] antiinfective,[16] antioxidative,[17] and antiproliferative[18] activities. Flavanones have attracted significant interest from chemists, biochemists, and pharmacologists due to their ample range of pharmacological activities and their uses as intermediates in the synthesis of various classes of bioactive compounds.

*Correspondence: drisraelenoch@gmail.com

Small molecules that bind to DNA are of 2 types: intercalating and nonintercalating. Intercalation into DNA consists of the binding molecules fitting between adjacent base pairs of DNA. The molecule is almost perpendicular to the DNA helix axis and is in close contact with the DNA base pairs.[19] Aromatic stacking interactions exist between the DNA base pairs and the dye molecule, and also occur between the DNA base pairs themselves. Nonintercalating dyes, due to bulkiness and other factors, bind to the outside of the double helical structure.[20] This occurs through groove binding or electrostatic binding. Groove binding involves molecules interacting with base pairs in either the major or minor grooves of DNA. This process widens the groove but does not elongate or unwind the double helix. In electrostatic binding, a cationic molecule is attracted to the anionic surface of DNA. These cations form ionic or hydrogen bonds along the outside of the DNA double helix.

In this paper we discuss (i) the mode and the strength of binding of flavanone (FL) with β-cyclodextrin (β-CD), and (ii) the effect of β-CD on the interaction of FL with calf thymus DNA (ctDNA), a model DNA. We explain that the selective blocking of the guest molecule, FL, by the host structure can lead to directing the mode of binding with DNA and that the host molecule can act as a vehicle to transport drugs onto DNA. We used 2D ROESY NMR for characterizing the structure of the host–guest complexes of FL with β-CD. Absorption spectroscopy, fluorescence spectroscopy, and molecular modeling were used for comprehending the mode and the strength of binding. Flavanone was chosen as it is the basic structural nucleus of the entire class of flavanones, which are of importance as explained earlier in this section.

2. Results and discussion

The chemical structures of flavanone and β-CD are shown in Figures 1a and 1b, respectively.

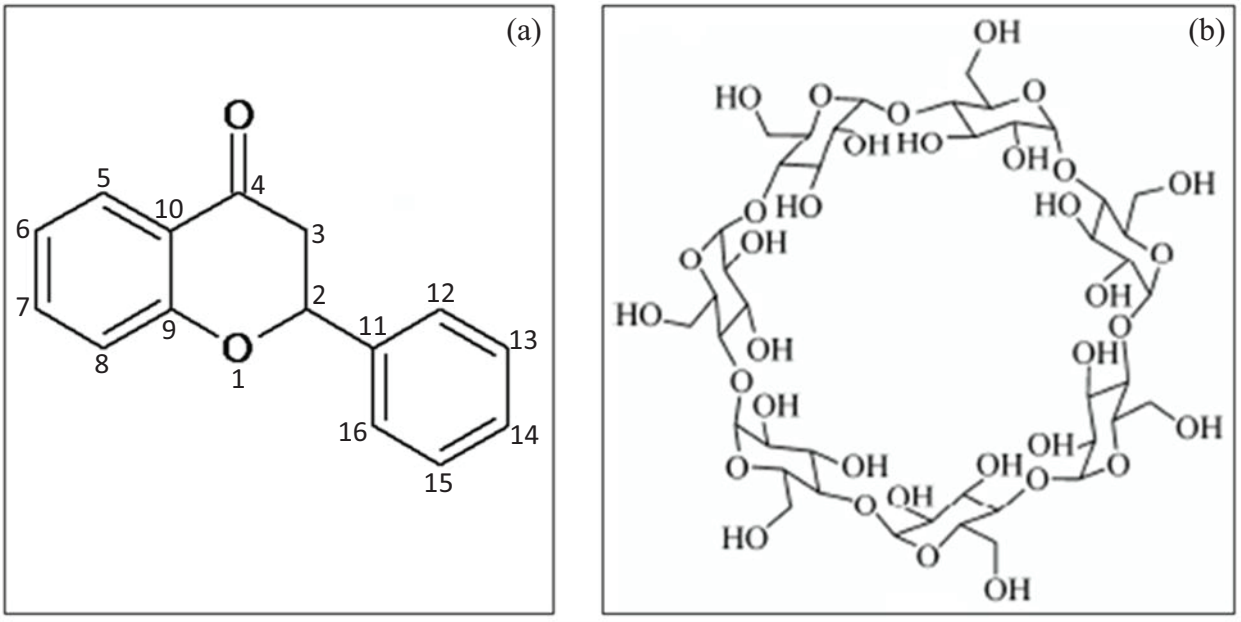

Figure 1. a) Structure of FL, b). Structure of β-CD.

2.1. Formation of the inclusion complex FL–β-CD

The inclusion complex formation of FL–β-CD was studied by keeping the concentration of FL fixed while that of β-CD varied from 0 to 1.2 $\times$ 10^{-2} mol dm^{-3}. The absorption spectra of FL with various concentrations

of aqueous β-CD are shown in Figure 2a. A hyperchromic effect was observed on the absorption bands at 254 and 321 nm upon the addition of β-CD solution with increasing concentration up to the maximum of 1.2×10^{-2} mol dm^{-3}. Moreover, a blue shift of absorbance from 321 to 318 nm was observed due to migration of the fluorophore from the polar environment to the nonpolar microenvironment inside the cavity of β-CD. The absorption maximum and absorbance data are given in Table 1. The plot of $1/(A - A_0)$ vs. $1/[\beta\text{-CD}]$ is shown in Figure 2b. The observed absorption spectral data were used in the following equation:

$$\frac{1}{A-A_0}=\frac{1}{A'-A_0}+\frac{1}{A'-A_0}\frac{1}{K[\beta-CD]} \tag{1}$$

Here A_0 is the absorbance of FL in water, A is the absorbance at each concentration of β-CD, and A$\prime$ is the intensity of absorbance at the highest concentration of β-CD. K is the binding constant. Linearity was observed in the plot with the observed correlation coefficient (R) of 0.99 and it suggested that there was formation of a 1:1 complex of FL–β-CD. The calculated binding constant (K) was 1449.28 mol^{-1} dm^3.

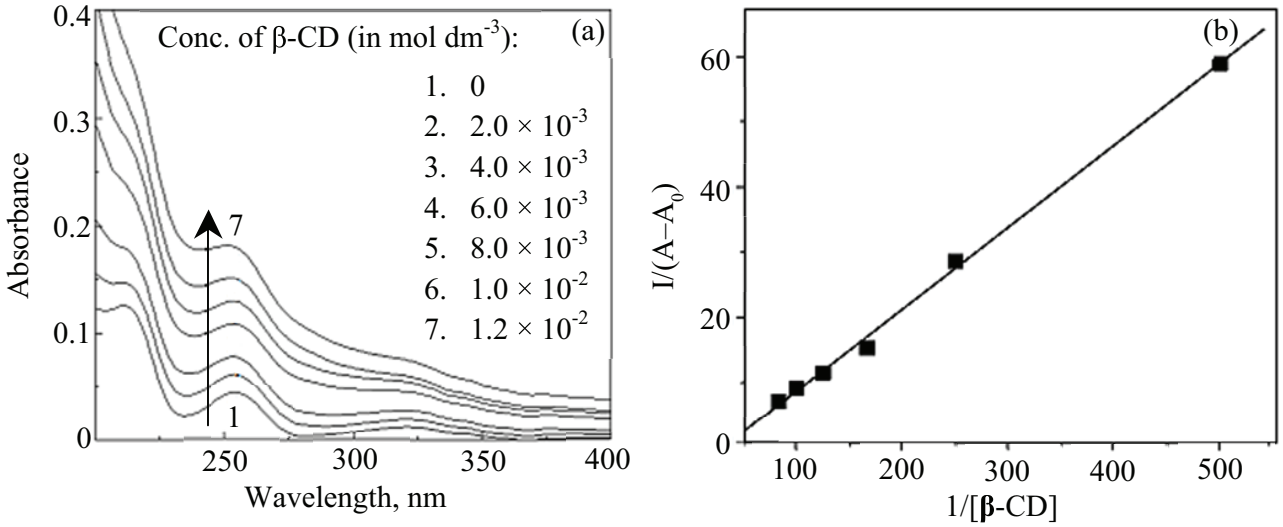

Figure 2. a) Absorption spectra of FL in varying concentrations of β-CD, b) Benesi–Hildebrand plot of FL/β-CD complex.

Table 1. Absorption and fluorescence spectral data of FL in various concentrations of β-CD.

Conc. of β-CD, mol dm^{-3}	Absorption maximum, nm	Absorbance	Fluorescence maximum, nm
0	321.0	0.0120	420.0
2.0×10^{-3}	321.0	0.0192	419.0
4.0×10^{-3}	320.0	0.0272	419.0
6.0×10^{-3}	320.0	0.0452	417.5
8.0×10^{-3}	319.0	0.0542	417.0
1.0×10^{-2}	319.0	0.0601	415.0
1.2×10^{-2}	318.0	0.0753	415.0

The fluorescence of FL was quenched upon the addition of β-CD, which might have been due to the formation of the FL–β-CD complex with the quenching of fluorescence observed upon each addition of β-CD

in aliquots. The fluorescence emission spectrum of the FL–β-CD complex is shown in Figure 3a. Addition of β-CD resulted in a large magnitude of quenching up to the concentration of 6.0×10^{-3} mol dm^{-3}. A significant blue shift, of the quenched fluorescence band, from 420 to 415 nm was observed and the emission maxima are given in Table 1. The Stern–Volmer plot between I_0/I and [β-CD] for the quenching of fluorescence is shown in Figure 3b. It was a nonlinear, downward concave curve that might be due to 2 fluorophore populations, 1 of which was not accessible to the quencher. The quenching might be explained as follows: at lower concentrations, the FL molecule was accessible by β-CD and the completion of the binding of FL with β-CD offered constraints to the accessibility of the FL molecules by excess β-CD molecules (above the concentration of β-CD, 6.0×10^{-3} mol dm^{-3}). However, these molecules could have partially had an interaction with FL and a much lower quenching rate was observed at higher concentrations of β-CD. Deviation from linearity in the Stern–Volmer plot might have occurred in line with the above phenomena. In such cases, the Stern–Volmer constant of the accessible fraction (K_a) can be determined from the equation.[21]

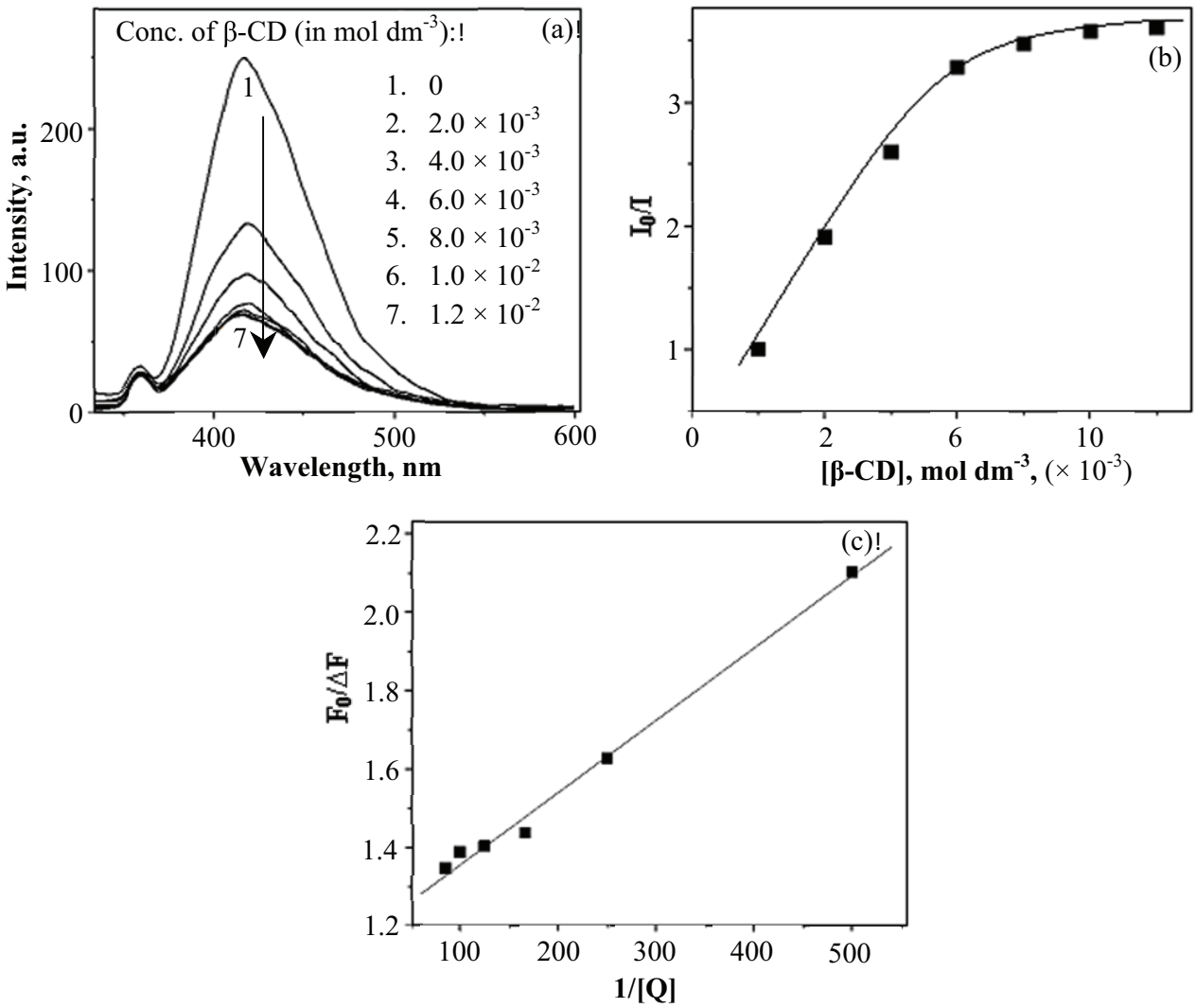

Figure 3. a) Fluorescence spectra of FL in varying concentrations of β-CD b) Stern–Volmer plot of FL/β-CD complex c) $F_0/\Delta F$ vs. 1/[Q] plot of FL/β-CD complex.

$$\frac{F_0}{\Delta F}=\frac{1}{f_a K_a [Q]}+\frac{1}{f_a}, \tag{2}$$

where f_a is the fraction of the initial fluorescence that remains accessible to the quencher. The modified form of the Stern–Volmer equation allowed f_a and K_a to be determined graphically as shown in Figure 3c. A plot of $F_0/\Delta F$ vs. $1/[Q]$ yields f_a^{-1} as the intercept and $(f_a K_a)^{-1}$ as the slope. The calculated Stern–Volmer constant of the accessible fraction was 461.61 mol^{-1} dm^3.

The time-resolved fluorescence decays of FL in water, and with low and high concentrations of β-CD are shown in Figure 4. The time-resolved fluorescence spectral data are given in Table 2. The decay profile of FL in water was bi-exponential, suggesting that it has emission originating from 2 excited states. One is from the locally excited state and the other from the more polar excited state. There was a decrease in the relative amplitude of the shorter lifetime species (T1). The relative amplitude of the longer lifetime (T2) species increased with an increase in the concentration of β-CD from 0 mol dm^{-3} to 1.2×10^{-3} mol dm^{-3}. The bi-exponential decay pattern, with 2 states of relative amplitudes 53.00 and 47.00, changes to the one having the final relative amplitudes of 39.71 and 60.29 at a maximal amount of the added β-CD (1.2×10^{-2} mol dm^{-3}). A systematic change in fluorescence lifetimes with an increase in the concentration of β-CD is an indication that a small fraction of the free FL and a greater amount of the FL–β-CD complex are present in solution. The marked decrease in the shorter lifetime was due to increased microviscosity caused by the added β-CD. In the excited state, microviscosity plays a predominant role compared to micropolarity.[22] The increase in the abundance of the species with a longer lifetime species in the presence of β-CD is due to the confinement effect offered to the guest (FL) within the β-CD cavity. When we added the third component to the fitted function, the χ^2 value did not improve. Hence, there should be 2 emitting species in solution with different individual

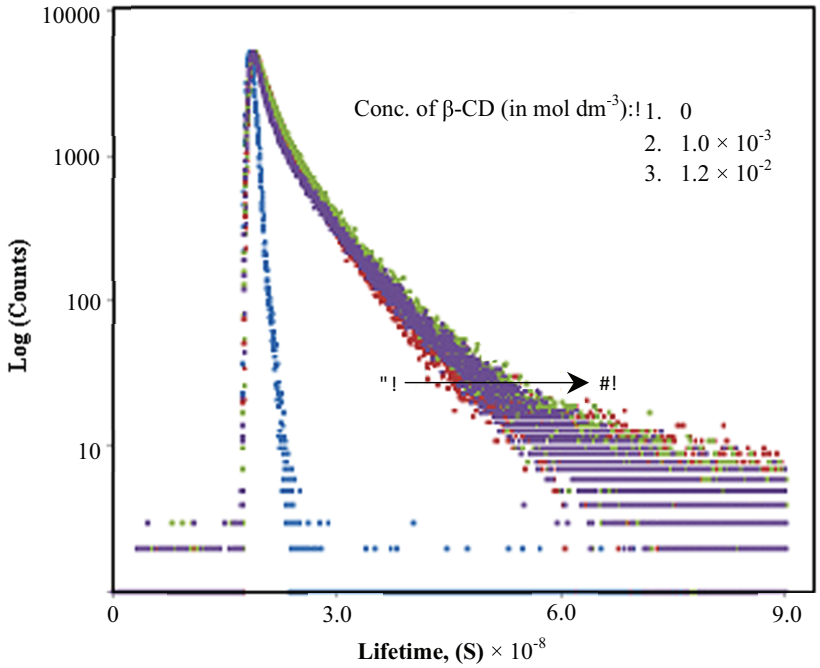

Figure 4. Time-resolved fluorescence spectra of FL in β-CD.

lifetimes. However, the lifetime of the complex did not change appreciably at high concentration of β-CD, suggesting that the complex–formation equilibrium was already shifted towards the complex side at much lower concentration of the added β-CD (1.0×10^{-3} mol dm^{-3}). In fact, compared to the concentration of FL, the concentration of the added β-CD was many-fold higher.

Table 2. Time-resolved fluorescence spectral data of FL in water and β-CD.

Conc. of β-CD mol dm^{-3}	Energy states	Lifetime (s)	Relative amplitude	χ^2	Standard deviation (s)
0	T1	2.0007×10^{-9}	53.00	1.0064	2.4519×10^{-11}
	T2	7.0122×10^{-9}	47.00		3.3750×10^{-11}
0.001	T1	1.4069×10^{-9}	40.76	1.1808	2.0047×10^{-11}
	T2	6.9222×10^{-9}	59.24		2.5906×10^{-11}
0.012	T1	9.2036×10^{-10}	39.71	1.0529	1.2184×10^{-11}
	T2	6.8713×10^{-9}	60.29		2.3467×10^{-11}

The formation of the inclusion complex of FL with β-CD was further confirmed by the NMR spectra of the inclusion complex. Table 3 lists the ^{1}H NMR chemical shifts of FL, β-CD, and FL–β-CD complex. The 2D ROESY NMR spectrum of the FL–β-CD complex is given in Figure 5. There were cross peaks observed for the protons of the methylene protons of the chromone (position 3) at the chemical shift of 2.83 ppm, and the aromatic protons 12 and 16 of FL at the chemical shift of 7.55 ppm in the abscissa showed cross correlation with the secondary hydroxyl protons of β-CD at 5.69 ppm and 5.74 ppm in the ordinate. These correlations occurred due to the inclusion of FL inside the hydrophobic cavity of the β-CD molecule with the phenyl ring at position 2 of the FL molecule getting encapsulated. This was further supported by the molecular modeling of FL with β-CD molecule. The molecular modeling poses of (A) hydrogen bonding, (B) hydrophobic, and (C) electrostatic interactions of FL to β-CD are shown in Figures 6a–c, respectively. A hydrogen bonding interaction occurred between the benzopyranone oxygen atom of FL and the hydrogen atoms of β-CD. The measured hydrogen bond lengths were (i) 2.114 Å for the bonding between hydrogen in the secondary hydroxyl group of β-CD and benzopyranone oxygen atom (O–H—O), (ii) 2.386 Å for the C–H—O bonding interaction.

Table 3. ^{1}H NMR spectral data of β–CD, FL, and FL–β-CD complex.

$\beta-$CD		FL			FL–β-CD complex
Position of protons	Chemical shift, δ (ppm)	Nature of proton	Position of protons	Chemical shift, δ (ppm)*	Chemical shift, δ (ppm)
H3	3.30	Benzo protons pyranone	Methylene protons H3	2.90; 3.10 (dd)	2.83; 2.88 (dd)
H4	3.33		H2	5.49 (dd)	5.56 (dd)
H2	3.56		H5 & H7	7.06 (m)	7.07 (m)
H6	3.60		H8	7.53 (d)	7.62 (d)
H5	3.64		H6	7.94 (dd)	7.80 (dd)
Primary hydroxyl protons	4.46	Phenyl protons	H12 & H16	7.51 (m)	7.55 (m)
H1	4.83		H13 & H15	7.44 (m)	7.44 (m)
Secondary hydroxyl protons	5.68, 5.74		H14	7.39 (m)	7.39 (m)

*dd – Doublet of doublets, d – Doublet, m – Multiplet

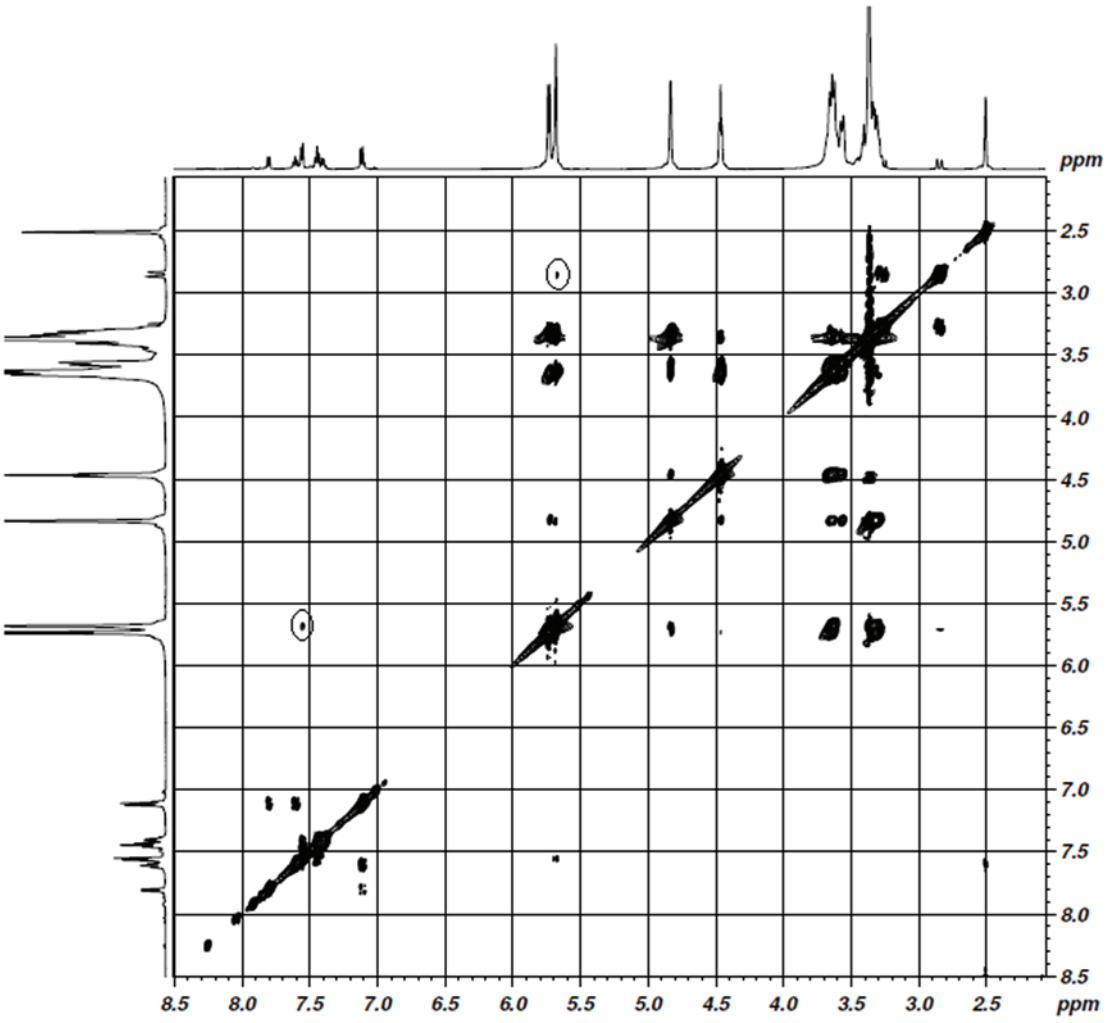

Figure 5. 2D ROESY NMR spectrum of FL/β-CD complex.

2.2. Binding studies of FL with β-CD/ctDNA

The FL molecule exhibited 2 absorption bands at 255 and 324 (Figure 7a). On the addition of ctDNA to the FL (at the concentration of 4×10^{-6} mol dm^{-3}), an increase in the absorption band at 255 nm and a decrease in the absorption band at 324 nm of FL were observed. An isosbestic point, at the wavelength of 301 nm, was observed in the absorption spectra corresponding to the interaction of FL with ctDNA. The binding constant, K, was evaluated as 2.32×10^5 mol^{-1} dm^3 (correlation coefficient, 0.98) with the plot of $A_0/(As - A_0)$ vs. 1/[DNA] for the interaction of FL with ctDNA (Figure 7b) by using the equation[23]

$$\frac{A_0}{A-A_0} = \frac{\varepsilon_G}{\varepsilon_{H-G}-\varepsilon_G} + \frac{\varepsilon_G}{\varepsilon_{H-G}-\varepsilon_G}\frac{1}{K[DNA]} \tag{3}$$

where A_0 and A are the absorbance of the free guest and the apparent one, and ε_G and ε_{H-G} are their absorption coefficients, respectively. The possibility of the presence of hydrogen and electrostatic interactions was optimized from the molecular modeling techniques. The modeling study showed that there was no

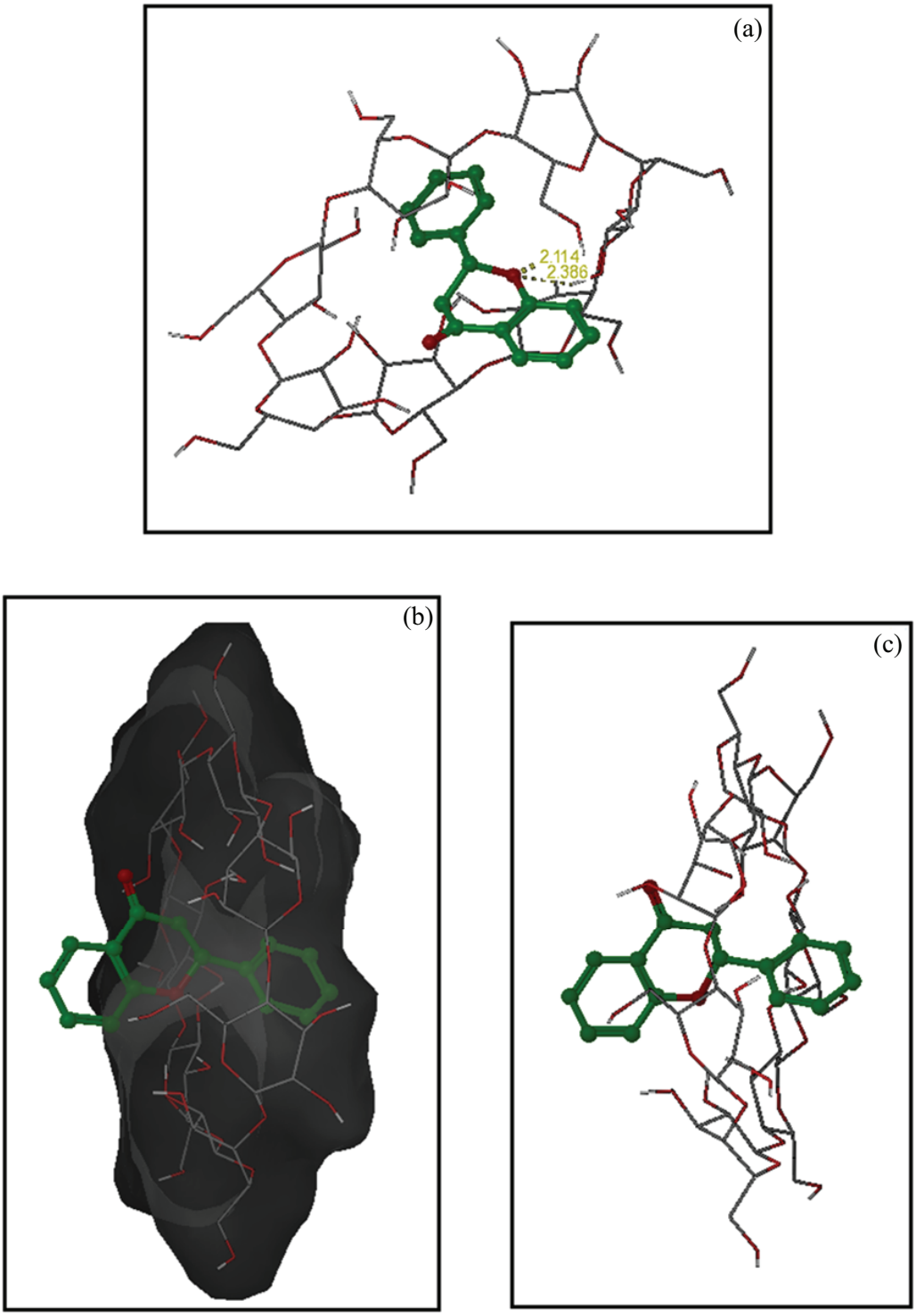

Figure 6. Molecular modeling poses of FL with a) Hydrogen bonding of β-CD b) Hydrophobic interaction of β-CD c) Electrostatic interaction of β-CD.

considerable interaction between the hydrophobic portion of FL and DNA. The possibility of hydrogen bonding between hydrogen of A8 nucleotide in the B strand of DNA and the bridged oxygen in the benzopyranone of FL (hydrogen bond length, 2.185 Å) is shown in Figure 8a. The electrostatic interaction between the benzopyranone parts of FL with DNA was observed as shown in Figure 8b. Thus the benzopyranone part of FL might be involved in the binding with DNA by means of hydrogen bonding and electrostatic interaction, respectively.

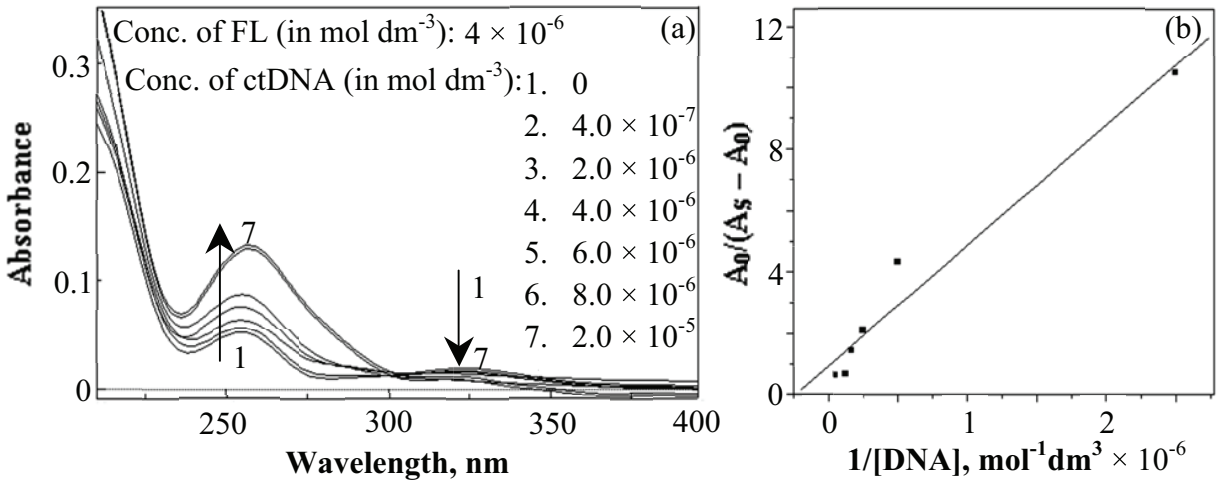

Figure 7. a) Absorption spectra of FL in varying concentrations of ctDNA b) Plot of 1/[DNA] vs. $A_0/(A_s - A_0)$.

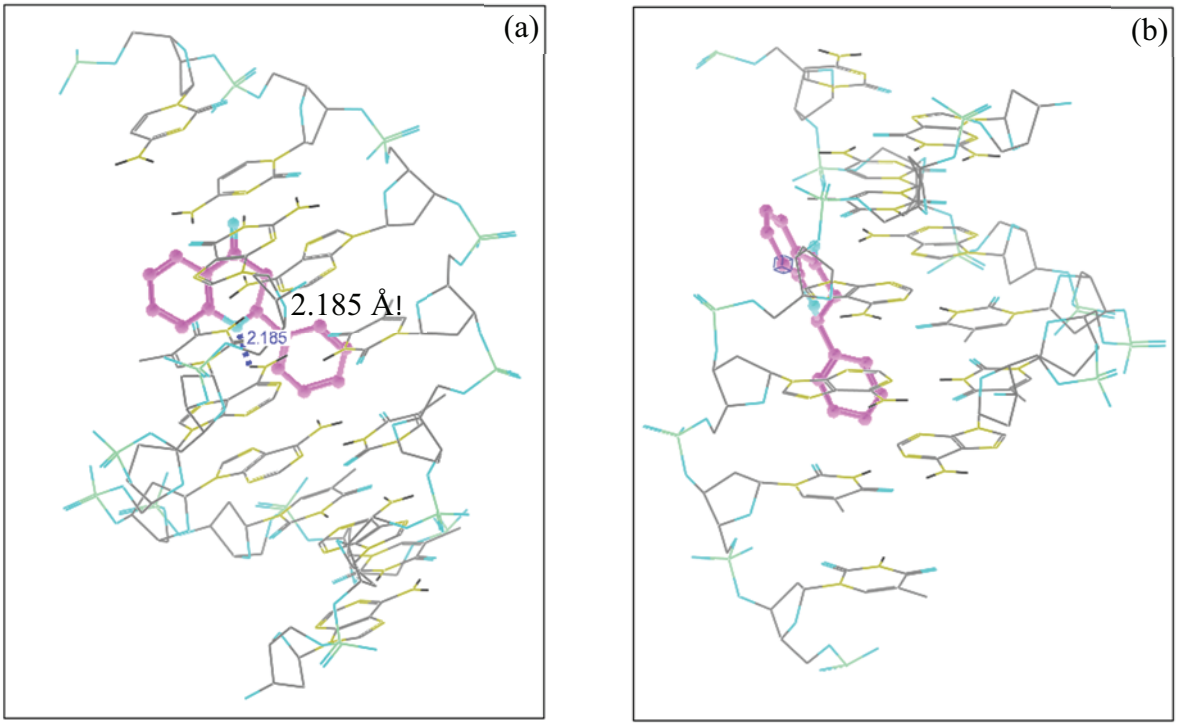

Figure 8. Molecular modeling poses of FL with a) Hydrogen bonding of DNA b) Electrostatic interaction of DNA.

The absorption bands of FL (4×10^{-6} mol dm^{-3}) were shifted to 254 and 314 nm in the presence of β-CD (4×10^{-3} mol dm^{-3}) as shown in Figure 9a. A considerable blue shift, $\approx$ 10 nm, of the phenyl ring of FL suggested the possible inclusion of the phenyl part of FL in β-CD. The addition of ctDNA to FL–β-CD resulted in an increase in the absorption of FL. The band at 314 nm was not affected due to the inclusion complexation of FL with β-CD through its phenyl substitution. Thus the benzopyranone part of FL, which contributed largely to the n–π^* transition at the longer wavelength absorption band, might have interacted with ctDNA. Using Eq. (2), the binding constant (K) was calculated as 1.13×10^5 mol^{-1} dm^3 (correlation coefficient, 0.99) for FL–β-CD interaction with ctDNA and the plot is given in Figure 9b. The benzopyranone group of FL was inferred to be involved in the interaction with DNA in both the absence and the presence of β-CD. A decrease in the binding affinity of FL–β-CD complex was observed with DNA due to the presence of β-CD. This might be because the inclusion complexation occurs through the phenyl substitution of FL with β-CD and makes the benzopyanone part available for the binding of DNA (Figure 10). A fluorescence spectral study was used to find the interaction of FL with ctDNA. The emission maximum λ_{emi} of FL was observed at 419 nm (Figure 11a). The binding titration of FL with ctDNA resulted in an increase in the fluorescence intensity of FL. There was no considerable shift in the emission maximum of FL upon the addition of ctDNA. This might be due to the electrostatic interaction of FL with ctDNA. In the presence of β-CD, a considerable blue shift of $\approx$2 nm was observed for FL (Figure 11b). The fluorescence intensity of FL (4×10^{-6} mol dm^{-3}) decreased approximately 36% from the original upon the addition of β-CD (4×10^{-3} mol dm^{-3}) (Figure 12). A significant enhancement in the fluorescence intensity of FL–β-CD was observed with the addition of ctDNA (Figure 12). The increase in the fluorescence intensity of FL and FL–β-CD with the interaction of ctDNA might be the result of the decrease in the collision frequency of the solvent molecules with FL molecules due to the stacking of the planar aromatic backbone of FL between the adjacent base pairs of ctDNA. Increasing of the molecule's planarity and decreasing of the collision frequency of solvent molecules with the complexes usually lead to emission enhancement.[24]

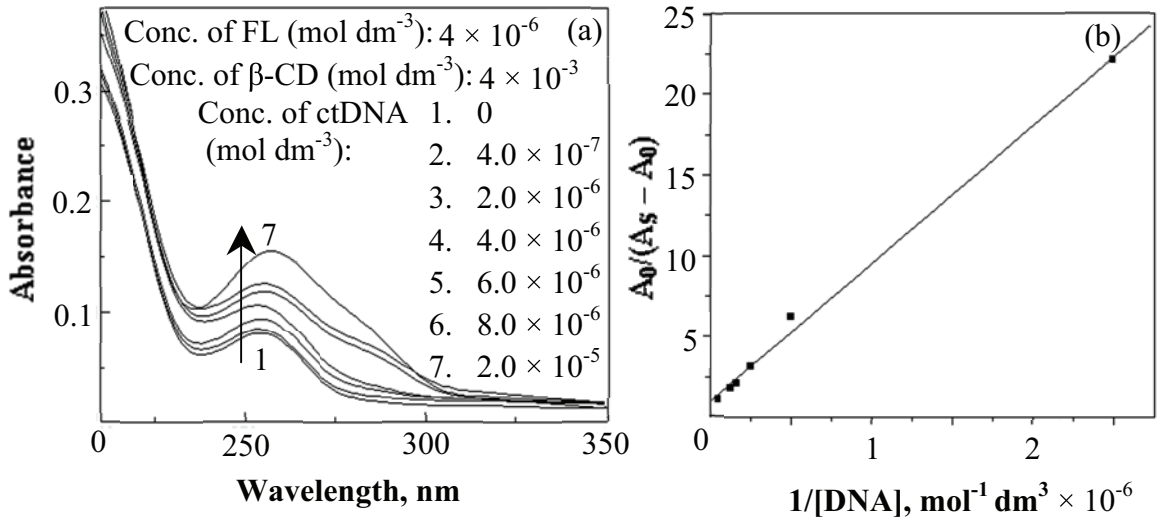

Figure 9. a) Absorption spectra of FL–β-CD in varying concentrations of ctDNA b) Plot of 1/[DNA] vs. $A_0/(A_s - A_0)$.

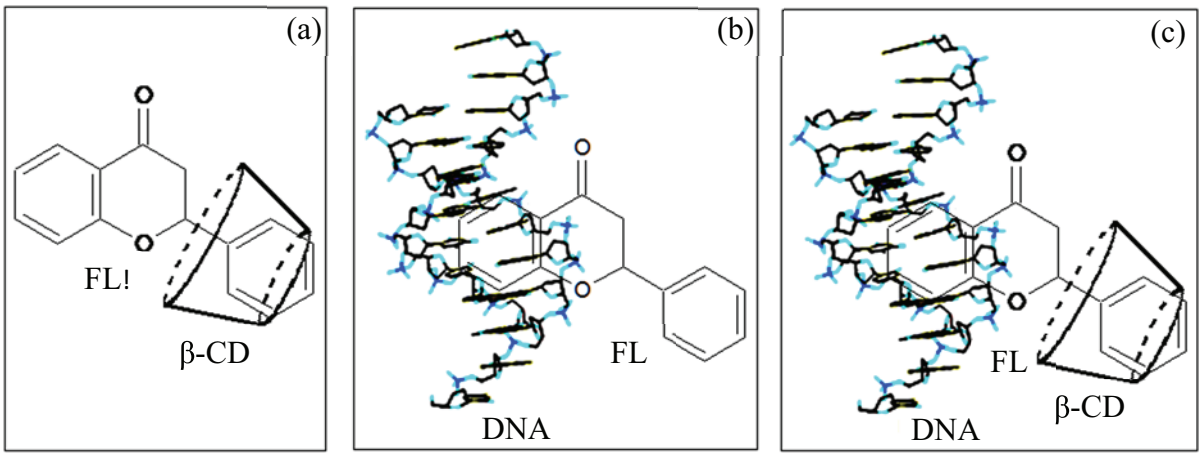

Figure 10. a) Structural representation of FL–β-CD complex b) Structural representation of binding of the FL with ctDNA c) Structural representation of binding of the FL–β-CD complex in ctDNA.

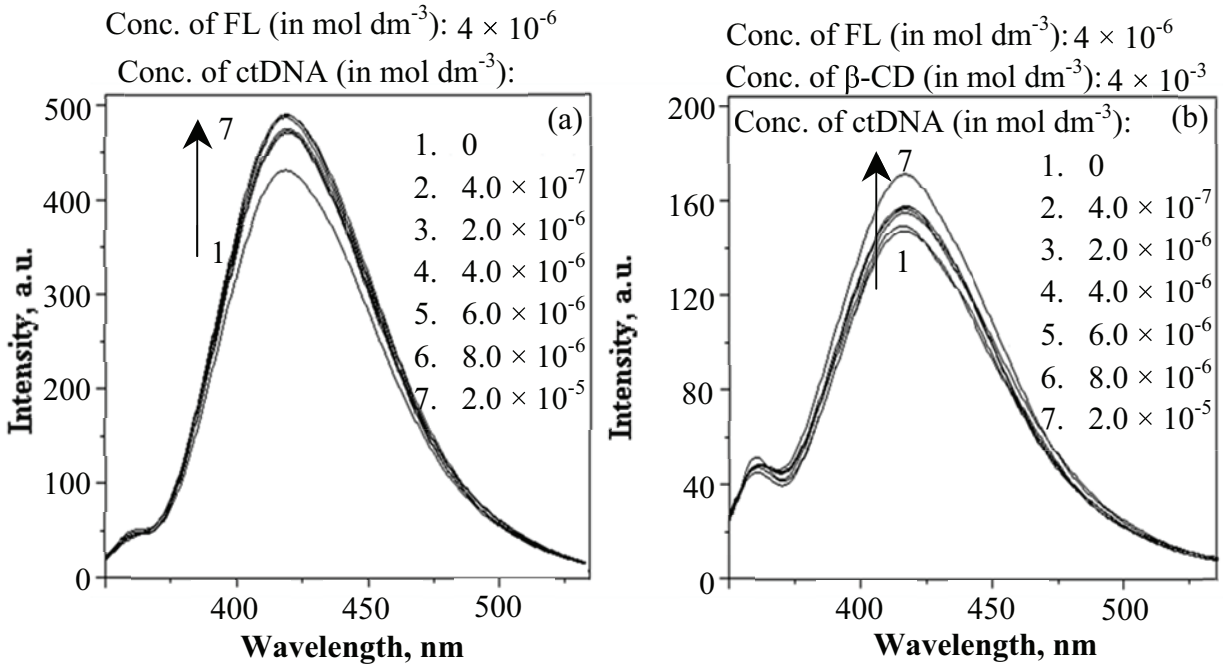

Figure 11. a) Fluorescence spectra of FL in varying concentrations of ctDNA b) Fluorescence spectra of FL–β-CD in varying concentrations of ctDNA.

3. Experimental section

3.1. Materials

Flavanone (purity 98%) was purchased from Sigma–Aldrich, India, and β-cyclodextrin (purity 98%) was bought from Hi Media, India. ctDNA (purity 90%) was purchased from Genei, Merck, India. These chemicals were used as received. All the solvents used from Merck were of spectral grade and were used as received without further purification.

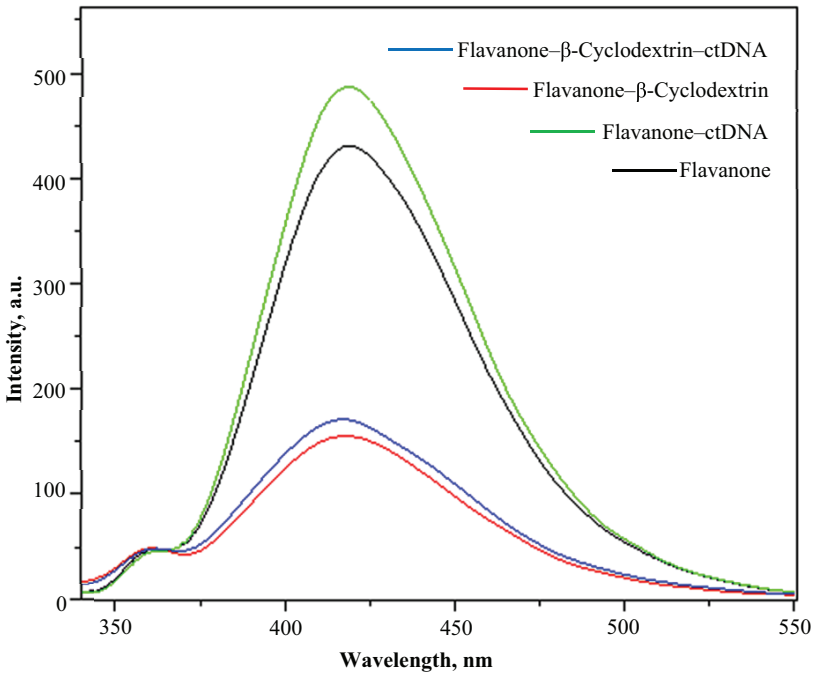

Figure 12. Fluorescence overlay spectrum of FL, FL–β-CD complex, FL–ctDNA binding, and FL–β-CD complex binding with ctDNA.

3.2. Methods

3.2.1. Preparation of FL–β-CD solid complex

FL (0.3 g, 1.34 $\times$ 10^{-3} mol) was dissolved in 5 mL of methanol and an equimolar amount of β-CD (1.52 g) was dissolved in 5 mL of doubly distilled water in 50-mL beakers separately. A solution of FL was added slowly to the solution of β-CD at room temperature and sonicated in an ultrasonicator for 30 min. The mixture was then warmed to 50 °C for 10 min and kept at room temperature for 2 days. The solid obtained was recrystallized from a methanol–water (1:1) mixture.

3.2.2. Preparation of test solutions

Test solutions were prepared by the appropriate dilution of stock solutions of FL and β-CD. Owing to the poor solubility of FL in water, the stock solution was made with methanol. In the test solutions the concentration of methanol was 1%. The purity of ctDNA was checked from optical measurements ($A_{260}/A_{280} > 1.8$, where A represents absorbance). ctDNA was dissolved in NaCl (50 mM) to obtain the desired concentration and acetate buffer solution (pH 3.5) was used to prepare the test solutions. Binding of FL to the β-CD–ctDNA was studied by the appropriate dilution of the stock solutions FL (1 $\times$ 10^{-4} mol dm^{-3}), β-CD (1.2 $\times$ 10^{-2} mol dm^{-3}), and ctDNA (2.3 $\times$ 10^{-4} mol dm^{-3}). All the experiments were carried out at an ambient temperature of 25 $\pm$ 2 °C. Homogeneous test solutions were obtained after the addition of all additives. The absorption and fluorescence spectrum were recorded against appropriate blank solutions.

3.2.3. Instrumentation

Absorption spectral measurements were performed using a double beam UV–visible spectrophotometer (Jasco V-630) using 1-cm path length cells. A spectrofluorimeter (PerkinElmer LS55), equipped with a 120-W xenon lamp for excitation, was used for the measurement of fluorescence. Both the excitation and the emission bandwidths were set up at 4 nm. Time-resolved fluorescence measurements were obtained on a time-correlated single photon counting HORIBA spectrofluorimeter using an LED source. An ultrasonicator, PCI 9L 250H (India), was used for sonication. 2D ROESY NMR spectra were recorded on a Bruker AV III instrument operating at 500 MHz with DMSO–d_6 as solvent for the FL–β-CD complex. Tetramethylsilane (TMS) was used as an internal standard. The chemical shift values were obtained downfield from TMS in parts per million (ppm). The mixing time for the ROESY spectra was 200 ms under the spin lock condition. The interaction of FL with β-CD and DNA was determined by molecular modeling using the software Schrödinger, Glide 5.5. B-DNA was used as a model for the theoretical studies. The structures of β-CD and duplex 5′-d(CCATTAATGG)$_2$-3′ were built and optimized by molecular mechanics.[25,26] The bond length and breadth of FL were calculated using Rasmol (Version 2.7.5.2) software[27] and the results are given in Figure 13.

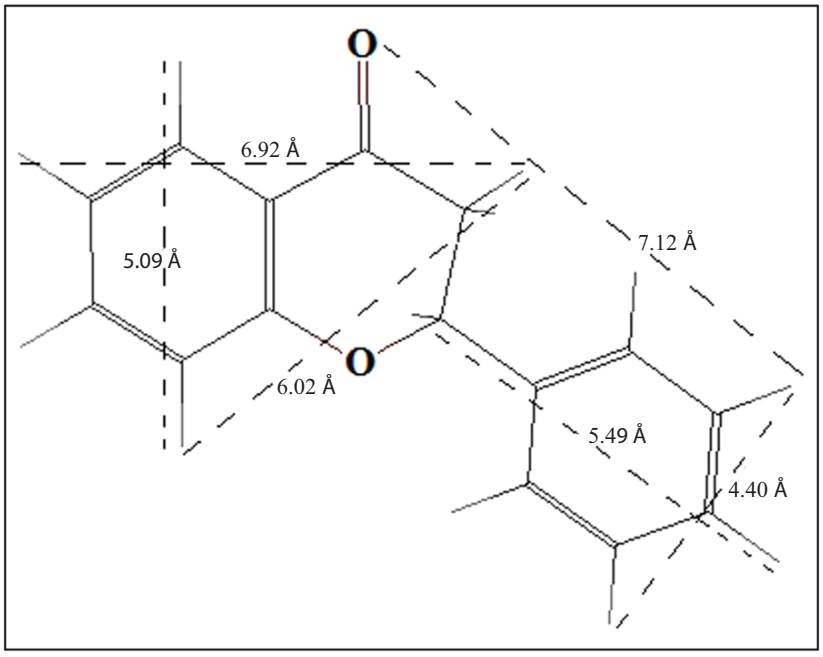

Figure 13.

4. Conclusions

Inclusion complexation of FL with β-CD occurs with a 1:1 stoichiometry with the phenyl group encapsulated with β-CD. The inclusion of the phenyl group of FL inside the cavity of β-CD is confirmed by the results obtained from absorptimetric titrations. The benzopyranone part of FL is involved in interaction with ctDNA in both the absence and the presence of β-CD. A decrease in the binding constant of FL with ctDNA is caused due to the presence of β-CD, which is driven by the inclusion complexation of the phenyl substitution of FL with β-CD. Thus, the β-CD acts as a carrier by the holding the phenyl group of FL and provides the benzopyranone part of FL for DNA binding. This can improve the availability of FL for binding with DNA.

Acknowledgment

The financial support of this study (SR/FT/CS-062/2009), by the Department of Science and Technology, Government of India, is gratefully acknowledged.

References

1. Shen, X.; Belletete, M.; Durocher, G. *J. Phys. Chem. B.* **1997**, *101*, 8212–8220.
2. Bender, M. L.; Komiyama, M. In *Cyclodextrin Chemistry*; Springer–Verlag: New York, NY, USA, 1978.
3. Saenger, W. *Angew. Chem., Int. Ed. Engl.* **1980**, *19*, 344–362.
4. Szejtli, J. In *Cyclodextrins and Their Inclusion Complexes*; Akademiai Kiado: Budapest, Hungary, 1982.
5. Li, S.; Purdy, W. C. *Chem. Rev.* **1992**, *92*, 1457–1470.
6. Szejtli, J. In *Cyclodextrin Technology*; Kluwer Academic Publishers: Dordrecht, Germany, 1988.
7. Yousuf, S.; Enoch I. V. M. V. *AAPS Pharm. Sci. Tech.* **2013**, *14*, 770–781.
8. Brewster, M. E.; Vandecruys, R.; Verreck, G.; Noppe, M.; Peeters, J. *J. Incl. Phenom. Macro. Chem.* **2002**, *44*, 35–38.
9. Enoch, I. V. M. V.; Yousuf, S. *J. Solution Chem.* **2013**, *42*, 470–484.
10. Stefansson, E.; Loftssonn, T. *J. Incl. Phenom. Macro. Chem.* **2002**, *44*, 23–27.
11. Boumendjel, A.; Ronot, X.; Boutonnat, J. *Curr. Drug Targets*, **2009**, *10*, 363–371.
12. Ducki, S. *Anticancer Agents Med. Chem.* **2009**, *9*, 336–347.
13. Kontogiorgis, C.; Mantzanidou, M.; Hadjipavlou-Litina, D. *Mini. Rev. Med. Chem.* **2008**, *8*, 1224–1242.
14. Tomar, V.; Bhattacharjee, G.; Kamaluddin, S.; Srivastava, R. K.; Puri, S. K. *Eur. J. Med. Chem.* **2010**, *45*, 745–751.
15. Mojzis, J.; Varinska, L.; Mojzisova, G.; Kostova, I.; Mirossay, L. *Pharmacol. Res.* **2008**, *57*, 259–265.
16. Sivakumar, P. M.; Priya, S.; Doble, M. *Chem. Biol. Drug. Des.* **2009**, *73*, 403–415.
17. Halfon, B.; Ciftci, E.; Topcu, G. *Turk. J. Chem.* **2013**, *37*, 464–472.
18. Pouget, C.; Lauthier F.; Simon, A.; Fagnere, C.; Basly, J. -P.; Delage, C.; Chulia, A. -J. *Bio-org. Med. Chem. Lett.* **2001**, *11*, 3095–3097.
19. Qu, X.; Ren, J.; Riccelli, P. V.; Benight, R.; Chaives, J. B. *Biochem.* **2003**, *42*, 11960–11967.
20. Pindur, U.; Jansen, M.; Lemster, T. *Curr. Med. Chem.* **2005**, *12*, 2805–2847.
21. Lakowicz, J. R. In *Principles of Fluorescence Spectroscopy*, 3rd ed., Springer, Singapore, 2000.
22. Panda, D.; Khatua, S.; Datta, A. *J. Phys. Chem. B* **2007**, *111*, 1648–1656.
23. Ibrahim, M. S.; Shehatta, I. S.; Al-Nayeli, A. A.; *J. Pharm. Biomed. Anal.* **2002**, *28*, 217–225.
24. Frezza, M.; Dou, Q. P.; Xiao, Y.; Samouei, H.; Rashidi, M.; Samari, F.; Hemmateenejad, B. *J. Med. Chem.* **2011**, *54*, 6166–6176.
25. Sameena, Y.; Enoch, I. V. M. V. *J. Lumin.* **2013**, *138*, 105–116.
26. Yan, L.; Ke, G.; Lv, J.; Gui S. Z., Qing, F. L. *J. Fluoresc.* **2011**, *21*, 409–414.
27. Bernstein, H. J. RasMol 2.7.5.2. Molecular graphics visualization tool. Based on RasMol 2.6 by Roger Sayle Biomolecular structures group. Stevenage, Hertfordshire, UK: Glaxo Welcome Research & Development, 2011.